Efficient Sum-of-Sinusoids-Based Simulation of Mobile Fading Channels with Asymmetrical Doppler Power Spectra

Carlos A. Gutiérrez-Díaz-de-León and Matthias Pätzold†

Faculty of Engineering and Science, Agder University College
P.O. Box 509, NO-4898 Grimstad, Norway
†matthias.paetzold@hia.no

***Abstract*— In this paper, we deal with the problem of designing efficient sum-of-sinusoids (SOS) based simulators for frequency non-selective mobile fading channels under non-isotropic scattering conditions. To cope with this problem, we propose a new parameter computation method that can be applied on any given asymmetrical Doppler power spectrum (DPS). With the aim to reduce the computational costs associated with the simulation of high-quality channel waveforms, we also present an efficient simulation approach that combines the proposed parameter computation method with the principle of set partitioning. By considering a reference model for a fading channel with asymmetrical DPS, it is shown that the resulting SOS-based channel simulator satisfactorily emulates the channel's autocorrelation function (ACF). Owing to its characteristics, the proposed channel simulation procedure proves to be a helpful tool for the test and performance analysis of modern wireless communication systems under non-isotropic scattering scenarios.**

I. Introduction

Mobile fading channel simulators based on the sum-of-sinusoids (SOS) principle introduced by Rice [1], [2] are nowadays widely in use for analyzing the performance of current and future wireless communication systems. For many years, this kind of channel simulators was one of the most important approaches for the simulation of narrow- and wideband wireless channels with specified time and frequency correlation functions [3]–[9]. More recently, the SOS principle has successfully been extended to enable the design of simulation models for space-selective wireless channels [10].

Various types of deterministic [3], [4] and stochastic [5]–[7] SOS-based channel simulation models have been proposed in the literature. All of them perform in general quite different and exhibit dissimilar statistical properties, as can be concluded from the research results presented in [4], [11], [12]. However, what almost all existing deterministic and stochastic SOS-based channel simulators have in common is that they have been developed mainly under the assumption of isotropic scattering, e.g., [3]–[9]. This poses a serious restriction, since modern wireless communication systems face non-isotropic scattering conditions.

To overcome the aforementioned restriction, we present a new parameter computation method that allows the design of SOS-based simulation models for non-isotropic scattering channels. The proposed method has been conceived to approximate the asymmetrical shape of the Doppler power spectrum (DPS) characterizing non-isotropic scattering environments. The resulting SOS-based channel simulator is deterministic [3], as all its parameters are constant quantities. In order to reduce the simulation expenditure associated with the generation of high-quality channel waveforms, we present an efficient simulation approach that combines the proposed parameter computation method with the principle of set partitioning, which was originally proposed in [13] for the case of isotropic scattering. In this paper, the procedure is extended to all kinds of non-isotropic scattering scenarios. The resulting simulation approach is quite advantageous, as it allows to improve the simulator's performance simply by averaging over several simulation trials.

It is important to stress that the simulation method described in this paper can be applied on any given (band-limited) DPS. However, to demonstrate the excellent performance of the proposed simulation technique, we present some exemplary numerical results obtained by applying our procedure on the reference model for a flat-fading channel with asymmetrical DPS derived in [14]. The results indicate that the designed SOS-based simulation model provides an efficient tool for simulating mobile fading channels with asymmetrical Doppler power spectra. We also present a performance comparison between our method and the L_p-norm method (LPNM) introduced in [15]. To the best of the authors' knowledge, the LPNM and the proposed method are the only parameter computation methods that allow the SOS-based simulation of non-isotropic scattering channels. The results let us conclude that the simulation techniques described in this paper are efficient alternatives to the LPNM.

The rest of the paper is organized as follows. Section II reviews the statistical properties of the reference and simulation models. Section III presents the proposed parameter computation method. Section IV explains how to combine this new method with the principle of set partitioning. Section V is devoted to the performance comparison between our method and the LPNM. Finally, Section VI concludes the paper.

II. The Reference and Simulation Models

A. The Reference Model

Our starting point is the mathematical description of a frequency non-selective Gaussian channel model for non-isotropic scattering environments. Such a channel model can be represented by a complex-valued Gaussian process

$$\mu(t) = \mu_{\mathrm{I}}(t) + j\mu_{\mathrm{Q}}(t), \quad j = \sqrt{-1} \tag{1}$$

with given correlation properties determined by an asymmetrical DPS. In (1), the inphase and quadrature components $\mu_{\mathrm{I}}(t)$ and $\mu_{\mathrm{Q}}(t)$ are real-valued Gaussian processes, each with zero mean and variance $\sigma^2/2$. This channel model is fully characterized by its autocorrelation function (ACF) $r_{\mu\mu}(\tau) := E\{\mu(t)^*\mu(t+\tau)\}$, or equivalently, by its DPS $S_{\mu\mu}(f)$, which is related to the ACF $r_{\mu\mu}(\tau)$ by the Fourier transform, i.e., $S_{\mu\mu}(f) = \int_{-\infty}^{\infty} r_{\mu\mu}(\tau)\exp\{-j2\pi f\tau\}d\tau$. The notation $E\{\cdot\}$ denotes statistical expectation, while $(\cdot)^*$ indicates complex conjugation. We assume throughout the paper that $\mu(t)$ has a band-limited DPS, so that $S_{\mu\mu}(f) = 0$ for $|f| \geq f_{\max}$, where $f_{\max}$ is the maximum Doppler frequency.

We recall that the inphase and quadrature components of $\mu(t)$ are uncorrelated processes if the scattering is isotropic. As a consequence, the DPS has a symmetrical shape with respect to the origin, i.e., $S_{\mu\mu}(f) = S_{\mu\mu}(-f)$. On the other hand, $\mu_{\mathrm{I}}(t)$ and $\mu_{\mathrm{Q}}(t)$ are correlated processes if the scattering is non-isotropic, which yields an asymmetrical DPS.

As an example, we consider the following asymmetrical DPS that was proposed in [14] for urban mobile radio channels

$$S_{\mu\mu}(f) = \frac{\sinh(\chi)}{\pi f_{\max}\sqrt{1-(f/f_{\max})^2}} \times \frac{\cosh(\chi) - f\cos(\phi_0)/f_{\max}}{[\cosh(\chi) - f\cos(\phi_0)/f_{\max}]^2 - [1-(f/f_{\max})^2]\sin^2(\phi_0)} \tag{2}$$

where $\sinh(\cdot)$ and $\cosh(\cdot)$ are the hyperbolic sine and cosine functions, respectively, and

$$\chi = \ln\left\{\left(1+\frac{1}{\gamma_0 d}\right) - \left[\left(1+\frac{1}{\gamma_0 d}\right)^2 - 1\right]^{1/2}\right\}. \tag{3}$$

The angle ϕ_0 determines the direction of the mobile terminal, γ_0 is the density of the buildings located in the propagation environment, and d is the distance between the base station and the mobile terminal.

Figure 1 shows the DPS $S_{\mu\mu}(f)$ in (2) for $f_{\max} = 91$ Hz, $\gamma_0 \cdot d = 10$, and different values of the direction angle ϕ_0. The asymmetry of the DPS can clearly be seen in this figure. The corresponding ACF of each of the graphs presented in Fig. 1 is shown in Fig. 2.

The channel model defined in (1) with the asymmetrical DPS in (2) constitutes our reference model.

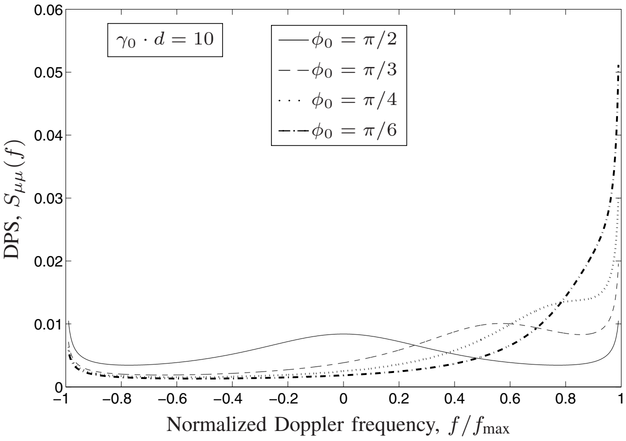

Fig. 1. DPS $S_{\mu\mu}(f)$ of the urban mobile fading channel model proposed in [14] for $f_{\max} = 91$ Hz, $\gamma_0 \cdot d = 10$, and different values of the direction angle ϕ_0.

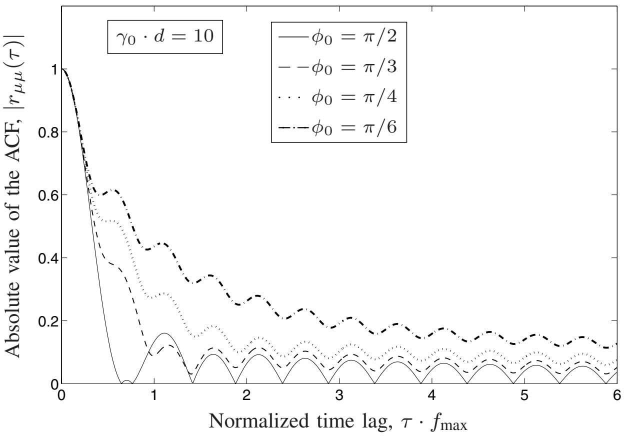

Fig. 2. Absolute value of the ACF $|r_{\mu\mu}(\tau)|$ of the urban mobile fading channel model proposed in [14] for $f_{\max} = 91$ Hz, $\gamma_0 \cdot d = 10$, and different values of the direction angle ϕ_0.

B. Simulation Model and Problem Description

Depending on the shape of $S_{\mu\mu}(f)$, the reference model is often an idealization of the physical channel, and therefore its exact hardware and/or software realization is generally not possible. Following the idea in [3], we can approximate the Gaussian process $\mu(t)$ in (1) by a deterministic complex SOS model

$$\tilde{\mu}(t) = \frac{\sigma}{\sqrt{N}} \sum_{n=1}^{N} \exp\{j(2\pi f_n t + \theta_n)\} \tag{4}$$

which represents our simulation model. In (4), the parameters N, f_n, and θ_n are constant quantities, which denote the number of harmonic waves, the nth Doppler frequency, and the nth Doppler phase, respectively. The performance of the simulation model strongly depends on the parameters N and f_n, while the Doppler phases θ_n have no significant influence on the statistics of $\tilde{\mu}(t)$.

The statistical properties of the simulation model described by $\tilde{\mu}(t)$, such as its mean value $\tilde{m}_\mu$, mean power (variance) $\tilde{\sigma}_\mu^2$, and ACF $\tilde{r}_{\mu\mu}(\tau)$, have to be obtained by means of time averages[1]. Bearing this in mind, one can show that $\tilde{m}_\mu := \langle \tilde{\mu}(t) \rangle = 0$ if $f_n \neq 0$ and $\tilde{\sigma}_\mu^2 := \langle |\tilde{\mu}(t) - \tilde{m}_\mu|^2 \rangle = \sigma^2$. In addition, it can be shown that the ACF $\tilde{r}_{\mu\mu}(\tau)$ can be expressed as

$$\begin{aligned} \tilde{r}_{\mu\mu}(\tau) &:= \lim_{T\to\infty} \frac{1}{2T} \int_{-T}^{T} \left[\tilde{\mu}(t)\right]^* \tilde{\mu}(t+\tau) dt \\ &= \frac{\sigma^2}{N} \sum_{n=1}^{N} \exp\{j2\pi f_n \tau\}. \end{aligned} \quad (5)$$

The Fourier transform of the ACF $\tilde{r}_{\mu\mu}(\tau)$ allows us readily to express the DPS $\tilde{S}_{\mu\mu}(f)$ of $\tilde{\mu}(t)$ in the form

$$\tilde{S}_{\mu\mu}(f) = \frac{\sigma^2}{N} \sum_{n=1}^{N} \delta(f - f_n). \quad (6)$$

Further details of the statistical properties of $\tilde{\mu}(t)$, such as the probability density function and level-crossing rate, can be found in [16]. Here it is only important to mention that the density of $\tilde{\zeta}(t) = |\tilde{\mu}(t)|$ is close to the Rayleigh distribution if $N \geq 10$.

From the results presented in this section, we may conclude that the problem at hand consists in finding the set of Doppler frequencies $\{f_n\}_{n=1}^{N}$ that produce the best possible approximation to the ACF $r_{\mu\mu}(\tau)$ of a given reference model $\mu(t)$.

III. The Proposed Parameter Computation Method

A. *The Modified Method of Equal Areas*

The application of the method of equal areas (MEA) [3], [15] on a given DPS $S_{\mu\mu}(f)$ allows us to compute the discrete Doppler frequencies f_n of the SOS model in (4) in such a way that the area under $S_{\mu\mu}(f)$ equals σ^2/N within the frequency range $f_{n-1} < f \leq f_n$. However, our investigations have shown that the performance of the MEA can be improved considerably if the relevant frequency range $(-f_{\max}, f_{\max}]$ is partitioned into $2N$ instead of N subintervals by points $x_0 = -f_{\max} < x_1 < x_2 < \ldots < x_{2N} = f_{\max}$, such that

$$\int_{x_{n-1}}^{x_n} S_{\mu\mu}(f) df = \frac{\sigma^2}{2N}, \quad n = 1, 2, \ldots, 2N. \quad (7)$$

Then the odd points x_{2n-1} are selected as Doppler frequencies f_n, i.e., $f_n = x_{2n-1}$ for $n = 1, 2, \ldots, N$. This slight but essential modification establishes the modified MEA (MMEA).

Repeating the calculations in [15, Sect. 5.1.3] for the MMEA results in the equation

$$\int_{-f_{\max}}^{f_n} S_{\mu\mu}(f) df = \frac{\sigma^2}{N} \left(n - \frac{1}{2}\right), \quad n = 1, 2, \ldots, N \quad (8)$$

from which the discrete Doppler frequencies f_n can be obtained for any given band-limited DPS $S_{\mu\mu}(f)$ by using numerical root-finding methods.

[1]The time average of a function $\chi(t)$ is denoted as $\langle \chi(t) \rangle$ and defined by $\langle \chi(t) \rangle := \lim_{T\to\infty} \frac{1}{2T} \int_{-T}^{T} \chi(t) dt$.

A closed-form solution of (8) can only be obtained if the inverse function G_f^{-1} of the cumulative power function

$$G_f(x) := \int_{-\infty}^{x} S_{\mu\mu}(f) df \quad (9)$$

exists. In this case, the MMEA results in

$$f_n = G_f^{-1}\left[\frac{\sigma^2}{N}\left(n - \frac{1}{2}\right)\right], \quad n = 1, 2, \ldots, N. \quad (10)$$

Note that if we replace $n - 1/2$ by n, then the MMEA corresponds to the MEA.

B. *Simulation Examples*

Figure 3 shows a comparison between the ACF $r_{\mu\mu}(\tau)$ of the reference model $\mu(t)$ and the ACF $\tilde{r}_{\mu\mu}(\tau)$ of the simulation model $\tilde{\mu}(t)$ obtained by using the MMEA with $N = 20$ and $\sigma^2 = 1$. We drew the graphs of the ACF of the reference model by employing numerical integration techniques to evaluate the inverse Fourier transform of the (normalized) DPS $S_{\mu\mu}(f)$ shown in (2). We considered four different propagation scenarios, which are characterized by the parameters $f_{\max} = 91$ Hz, $\gamma_0 \cdot d = 10$, and $\phi_0 = \{\pi/2, \pi/3, \pi/4, \pi/6\}$. The Doppler frequencies f_n were computed by solving (8) with the aid of numerical root-finding techniques. The results presented in Fig. 3 illustrate the good performance of the MMEA.

IV. Efficient Generation of High-Quality Channel Waveforms

In order to improve the performance of the SOS-based channel simulator, we could increase the number of complex harmonic functions, but this would increase the computational costs. The performance of typical deterministic SOS-based simulation models can only be improved in this manner [3], [4], [15]. Fortunately, it was recently shown in [13] that a simulation approach based on set partitioning allows to improve the performance simply by averaging over several simulation runs. Following the idea presented in [13], we explain here how to combine the MMEA with the principle of set partitioning to efficiently generate high-quality complex channel waveforms.

A. *The Modified Method of Equal Areas with Set Partitioning*

Basically, the idea consists in generating successively K uncorrelated complex waveforms

$$\tilde{\mu}^{(k)}(t) = \frac{\sigma}{\sqrt{N}} \sum_{n=1}^{N} \exp\{j(2\pi f_n^{(k)} t + \theta_n^{(k)})\}, \quad k = 1, \ldots, K \quad (11)$$

such that the sample mean ACF $\bar{r}_{\mu\mu}(\tau)$ [see (12)] equals the ACF $\tilde{r}_{\mu\mu}(\tau)$ of a single waveform $\tilde{\mu}(t)$ designed by using the MMEA with NK complex harmonic functions. Thereby, instead of simulating a single waveform $\tilde{\mu}(t)$ consisting of NK complex harmonic functions, one can alternatively perform K simulation trials of the waveforms $\tilde{\mu}^{(k)}(t)$, where each of these waveforms consists of only N complex harmonic functions. It is worth noticing that non-ergodic stochastic SOS-based

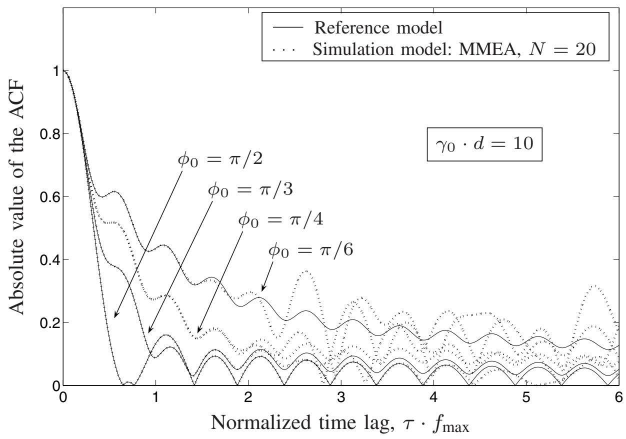

Fig. 3. Comparison between the absolute value of the ACF $|r_{\mu\mu}(\tau)|$ of the reference model $\mu(t)$ and the absolute value of the ACF $|\tilde{r}_{\mu\mu}(\tau)|$ of the simulation model $\tilde{\mu}(t)$ obtained by using the MMEA with $N = 20$, $f_{\max} = 91$ Hz and $\sigma^2 = 1$.

simulators, such as Monte Carlo simulators [5]–[7], depend also on the averaging of several simulation runs in order to asymptotically converge to the ACF of the reference model.

We define the sample mean ACF $\bar{r}_{\mu\mu}(\tau)$ as

$$\bar{r}_{\mu\mu}(\tau) := \frac{1}{K}\sum_{k=1}^{K} \tilde{r}^{(k)}_{\mu\mu}(\tau) \tag{12}$$

where $\tilde{r}^{(k)}_{\mu\mu}(\tau)$ is the ACF of the kth waveform $\tilde{\mu}^{(k)}(t)$. The cross-correlation function (CCF) $\tilde{r}^{(k,l)}_{\mu\mu}(\tau)$ between the kth waveform $\tilde{\mu}^{(k)}(t)$ and the lth waveform $\tilde{\mu}^{(l)}(t)$ is defined as

$$\tilde{r}^{(k,l)}_{\mu\mu}(\tau) := \lim_{T\to\infty} \frac{1}{2T}\int_{-T}^{T} \left[\tilde{\mu}^{(k)}(t)\right]^* \tilde{\mu}^{(l)}(t+\tau)dt. \tag{13}$$

Notice that the ACF $\tilde{r}^{(k)}_{\mu\mu}(\tau)$ of $\tilde{\mu}^{(k)}(t)$ follows from the CCF $\tilde{r}^{(k,l)}_{\mu\mu}(\tau)$ if $k = l$.

In brief, the aforementioned idea entails the fulfillment of the following two conditions:

$$(i) \qquad \bar{r}_{\mu\mu}(\tau) = \tilde{r}_{\mu\mu}(\tau), \qquad -\infty \le \tau \le \infty \tag{14}$$

$$(ii) \qquad \tilde{r}^{(k,l)}_{\mu\mu}(\tau) = 0, \qquad k \neq l \tag{15}$$

for $1 \le k \le l \le K$. In (14), $\tilde{r}_{\mu\mu}(\tau)$ is the ACF of a waveform $\tilde{\mu}(t)$ obtained by using the MMEA with $M = NK$ complex harmonic functions. It can be demonstrated that the Condition (ii) is satisfied by computing the Doppler frequencies such that

$$\{f^{(k)}_n\}_{n=1}^{N} \cap \{f^{(l)}_m\}_{m=1}^{N} = \{\emptyset\}, \quad \text{for } k \neq l. \tag{16}$$

In turn, for the equality in (14) to hold, it is necessary that

$$\bigcup_{k=1}^{K} \{f^{(k)}_n\}_{n=1}^{N} = \{f_m\}_{m=1}^{M=NK} \tag{17}$$

where $\{f_m\}_{m=1}^{M=NK}$ is the set of Doppler frequencies obtained by using the MMEA with $M = NK$ complex harmonic functions.

In the Appendix, it is shown that the Doppler frequencies $f^{(k)}_n$ of the kth waveform $\tilde{\mu}^{(k)}(t)$ can be obtained by numerically solving

$$\int_{-f_{\max}}^{f^{(k)}_n} S_{\mu\mu}(f)df = \frac{\sigma^2}{N}\left(n - \frac{1}{2}\right) + \epsilon_k, \quad n = 1, \ldots, N \tag{18}$$

where the shifting variable ϵ_k is given as

$$\epsilon_k = \frac{\sigma^2}{KN}\left(k - \frac{K+1}{2}\right) \tag{19}$$

for $k = 1, \ldots, K$. The role of the shifting variable ϵ_k is basically to guarantee the fulfillment of the Conditions (i) and (ii). Again, if the inverse of the cumulative power function $G_f(x)$ given in (9) exists, then we can compute the Doppler frequencies $f^{(n)}_n$ in closed form as

$$f^{(k)}_n = G_f^{-1}\left(\frac{\sigma^2}{N}\left[n - \frac{1}{2}\right] + \epsilon_k\right), \quad n = 1, \ldots, N \tag{20}$$

for $k = 1, \ldots, K$. We call this new parameter computation method the MMEA with set partitioning (MMEA-SP).

When the reference model is the DPS introduced by Jakes [17] for isotropic scattering scenarios, then the MMEA-SP reduces to the parameter computation method proposed in [13]. This is a very important feature of the MMEA-SP, since the method proposed in [13] leads to the best-known approximation of the Jakes DPS.

B. Performance Evaluation of the MMEA-SP

To demonstrate the advantages of the MMEA-SP, we compare in Fig. 4 the sample mean ACF of four ($K = 4$) uncorrelated waveforms $\tilde{\mu}^{(k)}(t)$, each with $N = 20$, and the ACF of the reference model under the same propagation scenarios considered in Fig. 3. We used the numerical approach [see (18)] to compute the Doppler frequencies of the four channel waveforms. We can observe from Fig. 4 that the sample mean ACF $\bar{r}_{\mu\mu}(\tau)$ of the four waveforms provides an excellent approximation of the ACF $r_{\mu\mu}(\tau)$ of the reference model over an interval that is K times larger than the one obtained by using the MMEA (cf. Fig. 3).

V. Comparison Between the MMEA-SP and the LPNM

As far as the authors are aware, the LPNM [15] was up to now the only parameter computation method suitable for the design of SOS-based simulation models for non-isotropic scattering channels. Actually, the LPNM was successfully employed in [10] for designing simulation models for multiple-input multiple-output (MIMO) wireless channels under non-isotropic scattering conditions.

Here, the LPNM is used to compute the Doppler frequencies f_n by minimizing the L_p-norm error function defined by [15]

$$E^{(p)}_{r_{\mu\mu}} := \left[\frac{1}{\tau_{\max}}\int_0^{\tau_{\max}} \left|r_{\mu\mu}(\tau) - \tilde{r}_{\mu\mu}(\tau)\right|^p d\tau\right]^{1/p} \tag{21}$$

where $\tau_{\max}$ establishes the interval $[0, \tau_{\max}]$ inside of which the approximation $\tilde{r}_{\mu\mu}(\tau) \approx r_{\mu\mu}(\tau)$ is of interest. Given the

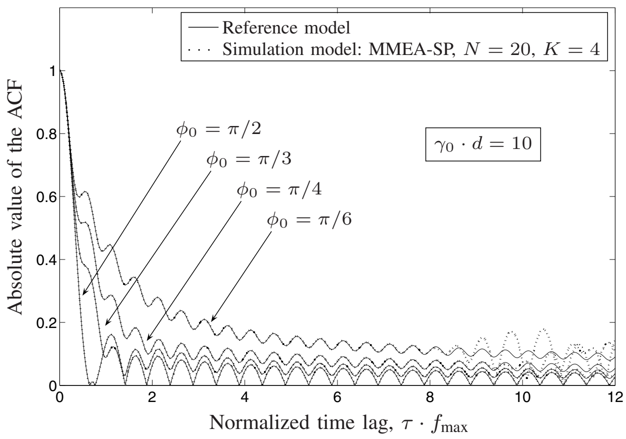

Fig. 4. Comparison between the absolute value of the ACF $|r_{\mu\mu}(\tau)|$ of the reference model and the absolute value of the sample mean ACF $|\bar{\mu}_{\mu\mu}(\tau)|$ of the simulation model by using the MMEA-SP with $N = 20$, $K = 4$, and $f_{\max} = 91$ Hz.

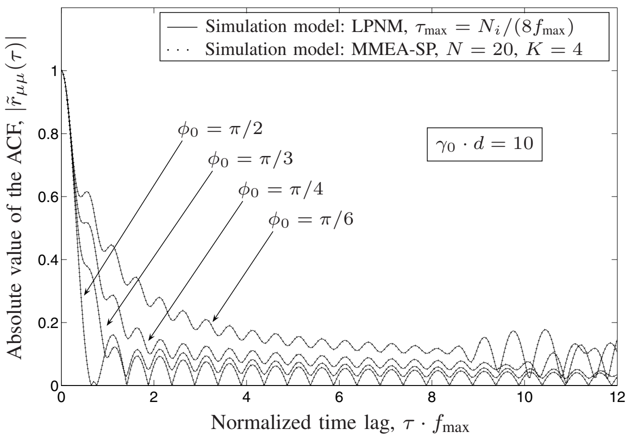

Fig. 5. Performance comparison between the MMEA-SP and the LPNM with respect to the ACF of the reference model proposed in [14].

computational burden of the minimization algorithm, it is of much importance to find out if the MMEA-SP constitutes an efficient alternative to the LPNM.

In order to find out whether the performance of the MMEA-SP measures up to that of the LPNM, we applied both methods to the channel model characterized by the asymmetrical DPS in (2). For the MMEA-SP, we considered the parameters $N = 20$ and $K = 4$, while we chose $p = 2$, $N = 80$, and $\tau_{\max} = N/(8 \cdot f_{\max})$ for the LPNM. The Doppler frequencies f_n obtained by using the MMEA with $N = 80$ were used as initial values for minimizing the error function $E^{(2)}_{r_{\mu\mu}}$. The results can be found in Fig. 5. This figure shows the absolute value of the simulation model's ACF, $|\tilde{r}_{\mu\mu}(\tau)|$, by using the MMEA-SP and the LPNM. We can observe from Fig. 5 that both methods have practically the same performance. This significant result allows us to conclude that the MMEA-SP (and also the MMEA) is an efficient alternative to the LPNM.

VI. Conclusions

In this paper, we presented a new parameter computation method for the design of complex SOS-based simulation models for non-isotropic scattering channels. The proposed method, which we have called MMEA, is quite general and can be applied to any given band-limited DPS. The simulation results obtained for the MMEA demonstrate its good performance. In addition, we presented an efficient simulation approach that combines the MMEA and the principle of set partitioning with the aim to reduce the computational costs caused by the generation of high-quality channel waveforms. The parameter computation method that results from such a combination has been named MMEA-SP. It has been shown here that the MMEA-SP improves the performance of the simulation model simply by averaging across several simulation runs. With regard to the performance comparison between the MMEA-SP and the LPNM, we found that the MMEA-SP produces a minimum in the L_p-norm error function when the statistical properties of the channel obey the analytical model proposed in [14] for urban mobile channels. The results of such a performance comparison let us conclude that the MMEA-SP (as well as the MMEA) constitutes an efficient and accurate alternative to the LPNM.

Appendix
Derivation of the Equations (18) and (19)

By noticing the requirement stated in (17), it turns out that the Doppler frequencies $\{f_n^{(k)}\}_{n=1}^N$ of the kth waveform $\tilde{\mu}^{(k)}(t)$ form a subset of the set composed by the Doppler frequencies $\{f_m\}_{m=1}^{M=NK}$ of a waveform $\tilde{\mu}(t)$ obtained by using the MMEA with $M = NK$ complex harmonic functions. Thus, in order to provide for each waveform $\tilde{\mu}^{(k)}(t)$ the best possible approximation to the ACF $r_{\mu\mu}(\tau)$ of the reference model $\mu(t)$ given that $\{f_n^{(k)}\}_{n=1}^N \subset \{f_m\}_{m=1}^{M=NK}$, we define

$$f_n^{(k)} = f_{k+(n-1)K}, \quad k = 1, \ldots, K \tag{22}$$

for $n = 1, \ldots, N$, where f_m is the mth Doppler frequency obtained by using the MMEA with $M = NK$ complex harmonic functions. From the conditions stated in (22) and using (8), we get

$$\begin{aligned} \int_{-f_{\max}}^{f_n^{(k)}} S_{\mu\mu}(f)df &= \int_{-f_{\max}}^{f_{k+(n-1)K}} S_{\mu\mu}(f)df \\ &= \frac{\sigma^2}{NK}\left(k + (n-1)K - \frac{1}{2}\right) \end{aligned} \tag{23}$$

for $n = 1, \ldots, N$ and $k = 1, 2, \ldots, K$. Finally, we rearrange the terms in (23) to obtain

$$\int_{-f_{\max}}^{f_n^{(k)}} S_{\mu\mu}(f)df = \frac{\sigma^2}{N}\left(n - \frac{1}{2}\right) + \epsilon_k \tag{24}$$

where

$$\epsilon_k = \frac{\sigma^2}{NK}\left(k - \frac{K+1}{2}\right). \tag{25}$$

Note that if $K = 1$, then $\epsilon_k = 0$, and thus the MMEA-SP reduces to the MMEA.

REFERENCES

[1] S. O. Rice, "Mathematical analysis of random noise," *Bell Syst. Tech. J.*, vol. 23, pp. 282-332, July 1944 .

[2] S. O. Rice, "Mathematical analysis of random noise," *Bell Syst. Tech. J.*, vol. 24, pp. 46-156, Jan. 1945 .

[3] M. Pätzold, U. Killat, and F. Laue, "A deterministic digital simulation model for Suzuki processes with application to a shadowed Rayleigh land mobile radio channel," *IEEE Trans. Veh. Tech.*, vol. 45, no. 2, pp. 318-331, May 1996.

[4] M. Pätzold, U. Killat, F. Laue, and Y. Li, "On the properties of deterministic simulation models for mobile fading channels," *IEEE Trans. Veh. Tech.*, vol. 47, no. 1, pp. 254-269, Feb. 1998.

[5] Y. R. Zheng, and C. Xiao, "Improved models for the generation of multiple uncorrelated Rayleigh fading waveforms," *IEEE Commun. Lett.*, vol. 6, no. 6, pp. 256-258, June 2002.

[6] —, "Simulation models with correct statistical properties for Rayleigh fading channels," *IEEE Trans. Commun.*, vol. 51, pp. 920928, June 2003.

[7] P. Höher, "A statistical discrete-time model for the WSSUS multipath channel," *IEEE Trans. Veh. Technol.*, vol. 41, no. 4, pp. 461-468, Nov. 1992.

[8] K.-W. Yip and T.-S. Ng, "Efficient simulation of digital transmission over WSSUS channels," *IEEE Trans. Commun.*, vol. 43, no. 12, pp. 2907-2913, Dec. 1995.

[9] C.-X. Wang, M. Pätzold, and Q. Yao, "Stochastic modeling and simulation of frequency-correlated wideband fading channels," *IEEE Trans. Veh. Technol.*, vol. 56, no. 3, pp. 1050-1063, May 2007.

[10] M. Pätzold and B. O. Hogstad, "A space-time simulator for MIMO channels based on the geometrical one-ring scattering model," *Wirel. Commun. Mob. Comput.*, vol. 4, pp. 727-737, 2004.

[11] C. S. Patel, G. L. Stüber, and T. G. Pratt, "Comparative analysis of statistical models for the simulation of Rayleigh faded cellular channels," *IEEE Trans. Commun.*, vol. 53, no. 6, pp. 1017-1026, June 2005.

[12] M. Pätzold, "On the stationarity and ergodicity of fading channel simulators based on Rice's sum-of-sinusoids," *Int. J. of Wireless Inf. and Networks*, vol. 11, no. 2, pp. 63-69, April 2004.

[13] M. Pätzold, B. O. Hogstad, and D. Kim, "A new design concept for high-performance fading channel simulators using set partitioning," *Wireless Personal Communications*, vol. 40, no. 2, pp. 267-279, Feb. 2007.

[14] N. Blaunstein, Y. Ben-Shimol, "Spectral properties of signal fading and Doppler spectra distribution in urban mobile communication links," *Wirel. Commun. Mob. Comput.*, vol. 6, no. 1, pp. 113-126, Feb. 2006.

[15] M. Pätzold, *Mobile Fading Channels*, Chichester, England: John Wiley and Sons, 2002.

[16] M. Pätzold and B. Talha, "On the statistical properties of sum-of-cisoids-based mobile radio channel simulators," in Proc. 10th International Symposium on Wireless Personal Multimedia Communications, WPMC 2007, Jaipur, India, Dec. 2007, submitted for publication.

[17] W. C. Jakes, *Microwave Mobile Communications*, Piscataway, NJ: IEEE Press, 1994.